Theoretical Study of the Reaction of Acetylene with BH_3, B_2H_6, and B_3H_7. A Proposed Mechanism of Carborane Formation

Michael L. McKee

Contribution from the Department of Chemistry, Auburn University, Auburn, Alabama 36849

Received December 12, 1994[⊗]

Abstract: The goal of this study is to evaluate a reaction mechanism which leads to the formation of a *closo*-carborane starting from $B_4H_{10} + C_2H_2$. Experimentally, it is known that alkylboranes, *nido*-carboranes, and *closo*-carboranes can all be obtained depending on reaction conditions. For this study, geometries were computed at the MP2/6-31G(d) level and relative energies were estimated at the [MP4/6-311+G(d,p)] level. The first assumed step is the elimination of BH_3 from B_4H_{10} to form B_3H_7. Rather than the expected hydroboration product, the initial reaction of $B_3H_7 + C_2H_2$ gives an addition product with little or no barrier. Loss of H_2 leads first to cyclic-$C_2B_3H_7$ carboranes and then through two methyleneborane intermediates to the known *nido*-$C_2B_3H_7$. Two pathways exist for loss of H_2 from *nido*-$C_2B_3H_7$, one synchronous and the other nonsynchronous, to the final product, 1,2-$C_2B_3H_5$. With respect to $B_4H_{10} + C_2H_2$, four activation barriers exist in the range 45−50 kcal/mol.

Introduction

The first evidence for carboranes was obtained in 1953 when Landesman[1] ignited mixtures of diborane and acetylene with a hot wire. The yield was less than 1%, but on the basis of positive-ion mass spectra, he identified fragments containing two carbons and three borons, two carbons and four borons, and two carbons and five borons. It was later found[2] that subjecting mixtures of B_5H_9 and C_2H_2 to a silent electrical discharge produced these same compounds but in better yields. On the basis of IR, NMR, and mass spectrometry, a closed polyhedron was suggested as the structure.[1]

The lower carboranes, $C_2B_5H_7$ and smaller, are usually prepared by reaction between lower boron hydrides and acetylenes.[3−8] Complex mixtures of alkylboranes, carboranes, and alkylcarboranes may be obtained, with the relative amounts of each dependent on the borane (B_2H_6, B_4H_{10}, or B_5H_9), the acetylene (C_2H_2, C_2HR, or C_2R_2), and the reaction conditions. Generally high-energy conditions[4,6] (e.g. silent electrical discharge or high temperatures) favor *closo*-carboranes, while low-energy conditions[4−8] (e.g. moderate heat) favor alkylboranes and *nido*-carboranes. For example, the reaction between diborane and acetylene gives ethyldiboranes if carried out at 85 °C[4] and a mixture of *closo*-carboranes if the gas mixture is subjected to an ac discharge.[3]

The best-known and well-studied reaction between a boron hydride and an unsaturated organic molecule is the hydroboration reaction.[10−13] Theoretical calculations of the type $HBR_2 + C_2H_4 \rightarrow R_2B-C_2H_5$ have been reported by several authors.[10−13] A π-complex has been found as an intermediate in the reaction at the semiempirical level[10] or at the HF level of ab initio theory.[11−13] When BH_3 is the reactant and electron correlation is included, the barrier for further reaction from the π-complex disappears,[14] while for alkylboranes (HBR_2), a π-complex exists at both the HF and post-HF levels.[12] The π-complex is much tighter and the transition state from the π-complex much "earlier" at the post-HF level compared to the HF level.[12] Variations on the hydroboration reaction have been reported where the inorganic reactant is B_2H_6 and $H_2O{\cdot}BH_3$. In the reactions of complexed BH_3, the BH_3 moiety must undergo partial dissociation before reaction can occur. These reactions can be viewed as either single steps ($R{\cdot}BH_3 \rightarrow R + BH_3$; $BH_3 + C_2H_4 \rightarrow H_2B-C_2H_5$) or two-step reactions ($R{\cdot}BH_3 \rightarrow R + BH_3$; $BH_3 + C_2H_4 \rightarrow H_2B-C_2H_5$). At lower temperatures, the single-step reaction has a lower free energy of activation, but at higher temperatures, the two-step mechanism is preferred.[12]

The reactions of BH_3 or B_2H_6 with alkynes have also been studied.[10,12] Houk and co-workers[12] found that for BH_3 addition to alkynes, the π-complex was weaker and the activation barrier larger compared to addition to alkenes. This observation is in keeping with expectations based on a higher IP for C_2H_2 relative to C_2H_4 (11.40 versus 10.51 eV) and with the experimental observation that double bonds are more reactive to BH_3 than triple bonds.[12]

Considerable effort has been expended to understand rearrangements in carboranes.[15−26] Carboranes formed from the

[⊗] Abstract published in *Advance ACS Abstracts*, July 1, 1995.

(1) For an excellent review see: Williams, R. E. Early Carboranes and Their Structural Legacy. In *Advances in Organometallic Chemistry*; Stone, F. G. A., West, R., Eds.; Academic Press: New York, 1994; Vol. 36, pp 1−55.

(2) Shapiro, I.; Keilin, B.; Good, C. D.; Williams, R. E. *J. Am. Chem. Soc.* **1963**, *85*, 3167.

(3) Grimes, R. N. *J. Am. Chem. Soc.* **1966**, *88*, 1895.

(4) Linder, H. H.; Onak, T. *J. Am. Chem. Soc.* **1966**, *88*, 1886.

(5) Grimes, R. N.; Bramlett, C. L. *J. Am. Chem. Soc.* **1967**, *89*, 2557.

(6) (a) Grimes, R. N.; Bramlett, C. L.; Vance, R. L. *Inorg. Chem.* **1968**, *7*, 1066. (b) Grimes, R. N.; Bramlett, C. L.; Vance, R. L. *Inorg. Chem.* **1969**, *8*, 55.

(7) Onak, T. P.; Dunks, G. B.; Spielman, J. R.; Gerhart, F. J.; Williams, R. E. *J. Am. Chem. Soc.* **1966**, *88*, 2061.

(8) Franz, D. A.; Grimes, R. N. *J. Am. Chem. Soc.* **1970**, *92*, 1438.

(9) Grimes, R. N. *Carboranes*; Academic Press: New York, 1970; pp 23−31.

(10) Dewar, M. J. S.; McKee, M. L. *Inorg. Chem.* **1978**, *17*, 1075.

(11) Clark, T.; Wilhelm, D.; Schleyer, P. v. R. *J. Chem. Soc., Chem. Commun.* **1983**, 606.

(12) Wang, X.; Li, Y.; Wu, Y.-D.; Paddon-Row, M. N.; Rondan, N. G.; Houk, K. N. *J. Org. Chem.* **1990**, *55*, 2601.

(13) Hommes, N. J. R. v. E.; Schleyer, P. v. R. *J. Org. Chem.* **1991**, *56*, 4074.

(14) At very high levels of theory (QCISD(T)/6-311+G**//QCISD/6-31G*), a barrier of 0.05 kcal/mol is calculated for further reaction from the π-complex.[13]

(15) Gimarc, B. M.; Ott, J. J. *Main Group Met. Chem.* **1989**, *12*, 77.

(16) Gimarc, B. M.; Ott, J. J. Graphs for Chemical Reaction Networks: Applications to the Carboranes. In *Graph Theory and Topology in Chemistry*; King, R. B., Rouvray, D. H., Eds.; Elsevier: Amsterdam, 1987; pp 285−301.

(17) Gimarc, B. M.; Daj, B.; Warren, D. S.; Ott, J. J. *J. Am. Chem. Soc.* **1990**, *112*, 2597.

(18) Mingos, D. M. P.; Wales, D. J. *Introduction to Cluster Chemistry*; Prentice Hall: Englewood Cliffs, NJ, 1990; pp 218−248.

0002-7863/95/1517-8001$09.00/0

reaction of acetylene with boron hydrides often have directly bonded carbon atoms which are kinetic products and rearrange to isomeric forms with nonadjacent carbons when subjected to elevated temperatures. Two well-known carborane examples are 1,2-$C_2B_4H_6$[26b,c] and 1,2-$C_2B_{10}H_{12}$.[27-29] The former rearranges to 1,6-$C_2B_4H_6$ at 300 °C while the latter rearranges first to 1,7-$C_2B_{10}H_{12}$ at 450 °C and then to 1,12-$C_2B_{10}H_{12}$ at 620 °C. Computational studies suggest that rearrangement in $C_2B_4H_6$ takes place via a benzvalene-like intermediate with an activation barrier of 35 kcal/mol.[26b,c] In a novel departure from this mechanism, Schleyer and co-workers[30] have considered an isomer of $C_2B_4H_6$ which could play a role in carborane combustion. The new $C_2B_4H_6$ isomer is based upon the $C_2B_3H_5$ pentagonal bipyramid with a BH_2 group replacing a hydrogen (i.e. $C_2B_3H_4-BH_2$).

In $C_2B_{10}H_{12}$, several mechanisms are possible. From arrangements in a series of tethered compounds, Wu and Jones[27] have deduced that the triangle-face rotation is the most likely mechanism, a conclusion which is supported by MNDO calculations in the isoelectronic $B_{12}H_{12}^{2-}$ system.[31] Edvenson and Gaines[28] proposed an open-cage transition state for the carborane rearrangement and demonstrated that other poroposed mechanisms were special cases of this *closo* → *nido* → *closo* mechanism. Most recently, Wales[29] studied the rearrangement at the STO-3G level. He found that lower-symmetry transition states were perferred, thereby effectively avoiding symmetry-forbidden pathways of higher symmetry.

Two overlapping general types of mechanism in *closo*-carboranes can be identified: the nonclassical → classical → nonclassical mechanism[32a] and the *closo* → *nido* → *closo* mechanism.[32b] The transition state/intermediate in the nonclassical → classical → nonclassical mechanism has a smaller number of multicenter bonds and a larger number of vacancies on boron atoms, while the transition state/intermediate in the *closo* → *nido* → *closo* mechanism adopts the geometry of a recognizable *nido*-carborane—usually a more open structure. The distinction between the two groups is not precise, especially since either mechanism may involve the Diamond–Square–Diamond (DSD) rearrangement[1] or a series of concerted DSD rearrangements. As an example of the latter mechanism, recent ab initio calculations were presented which demonstrated a low-energy pathway through a *nido* structure for rearrangement in $C_2B_7H_9$.[33]

From a computational study of rearrangement mechanisms in $C_2B_3H_5$[26a] and $C_2B_5H_7$,[26b,c] the concerted double diamond–square–diamond mechanism (or local bond rotation) was considered to be a low-energy pathway. Some rearrangement mechanisms have high activation barriers because they involve a HOMO-LUMO crossing.[34] Using graph theory[16] Tensor Surface Harmonics (TSH) theory,[18-20] rules have been developed for predicting when crossings will occur in the rearrangement of carboranes.

Our understanding of rearrangements in the carboranes is substantially more advanced than our understanding of their formation. The two routes depicted in eqs 1 and 2 for formation

$$B_4H_{10} + C_2H_2 \xrightarrow{\text{(silent electric discharge)}} 1-2\%\ C_2B_3H_5 \quad (1)$$

$$B_4H_{10} + C_2H_2 \xrightarrow{\Delta\ (50\ ^\circ C)} 1,2\text{-}C_2B_3H_7,\ 2,3\text{-}C_2B_4H_8,\ C_3B_3H_7 \quad (2)$$

of carborane represent very different reaction conditions.[35] The silent electric discharge in eq 1 generates a plasma which yields very reactive species and locally high thermal energies which should favor fragmentation pathways over condensation pathways. Equation 2, on the other hand, takes place with mild heating.

The first likely step in either reaction is the decomposition of B_4H_{10} to give B_3H_7 (eq 3a) or B_4H_8 (eq 3b) followed by

$$B_4H_{10} \rightarrow B_3H_7 + BH_3 \quad (3a)$$

$$B_4H_{10} \rightarrow B_4H_8 + H_2 \quad (3b)$$

addition of C_2H_2 to the reactive boron hydride. The present work will consider the addition of B_3H_7 to C_2H_2, while a subsequent paper will deal with reactions of B_4H_8 with C_2H_2. The most straightforward mechanism would involve an addition complex followed by the successive loss of two hydrogen molecules (eqs 4–6). The details of this mechanism will be considered in this work.

$$B_3H_7 + C_2H_2 \rightarrow C_2B_3H_9 \quad (4)$$

$$C_2B_3H_9 \rightarrow C_2B_3H_7 + H_2 \quad (5)$$

$$C_2B_3H_7 \rightarrow C_2B_3H_5 + H_2 \quad (6)$$

The actual mechanism of carborane formation, no doubt, involves a complex series of competing reactions. This work will follow one possible thread from reactants to products. Except for the addition of acetylene, all reactions considered will be unimolecular reactions and all products will have one C–C bond.

An interesting isoelectronic variation of eq 4 is shown in eq 7, which produces a μ-aminodiborane(6) derivative in what must

$$\begin{matrix} THF{\cdot}B_3H_7 + (R = t\text{Bu}) \rightarrow \mu\text{-}(HRN)B_2H_4R \\ RB{\equiv}NR \end{matrix} \quad (7)$$

be a multistep reaction.[36] The reaction product in eq 7 has no analogy in the $B_3H_7 + C_2H_2$ reaction, which is probably because the reaction takes place in THF solution at room temperature,

(19) Mingos, D. M. P.; Wales, D. J. Skeletal Rearrangements in Clusters: Some New Theoretical Insights Involving Lipscomb's Diamond-Square-Diamond Mechanism. In *Electron Deficient Boron and Carbon Clusters*; Olah, G. A., Wade, K., Williams, R. E., Eds.; Wiley: New York, 1991; pp 143–163.
(20) Wales, D. J.; Bone, R. G. A. *J. Am. Chem. Soc.* **1992**, *114*, 5399.
(21) For a detailed example of rearrangement in *nido*-B_6H_{10} see: Mebel, A. M.; Morokuma, K.; Musaev, D. G. *J. Am. Chem. Soc.* **1994**, *116*, 3932.
(22) For related rearrangements of boron hydrides see: (a) Gaines, D. F.; Coons, D. E.; Heppert, J. A. The Elucidation of Cluster Rearrangement Mechanisms Using Isotopically Labeled Boron Hydrides. In *Molecular Structure and Energetics. Advances in Boron and the Boranes*; Liebman, J. F., Greenberg, A. G., Williams, R. E., Eds.; VCH: New York, 1988; pp 91–104. (b) Greenwood, N. N. *Chem. Soc. Rev.* **1992**, 49.
(23) Williams, R. E. *Chem. Rev.* **1992**, *92*, 177.
(24) Štíbr, B. *Chem. Rev.* **1992**, *92*, 225.
(25) Heřmánek, S. *Chem. Rev.* **1992**, *92*, 325.
(26) (a) McKee, M. L. *THEOCHEM* **1988**, *168*, 191. (b) McKee, M. L. *J. Am. Chem. Soc.* **1988**, *110*, 5317. (c) McKee, M. L. *J. Am. Chem. Soc.* **1992**, *114*, 879.
(27) Wu, S.; Jones, M. *J. Am. Chem. Soc.* **1989**, *111*, 5373.
(28) Edvenson, G. M.; Gaines, D. F. *Inorg. Chem.* **1990**, *29*, 1210.
(29) Wales, D. J. *J. Am. Chem. Soc.* **1993**, *115*, 1557.
(30) Slutsky, V. G.; Hofmann, M.; Schleyer, P. v. R. *Mendeleev Commun.* **1994**, 12.
(31) Dewar, M. J. S.; McKee, M. L. *Inorg. Chem.* **1978**, *17*, 1569.
(32) (a) Graham, G. D.; Marynick, D. S.; Lipscomb, W. N. *J. Am. Chem. Soc.* **1980**, *102*, 2939. (b) Wong, H. S.; Lipscomb, W. N. *Inorg. Chem.* **1975**, *14*, 1350.
(33) Ceulemans, A.; Goijens, G.; Nguyen, M. T. *J. Am. Chem. Soc.* **1994**, *116*, 9395.
(34) (a) Gimarc, B. M.; Ott, J. J. *Inorg. Chem.* **1986**, *25*, 83. (b) Gimarc, B. M.; Ott, J. J. *Inorg. Chem.* **1986**, *25*, 2708. (c) Gimarc, B. M.; Ott, J. J. *J. Comput. Chem.* **1986**, *7*, 673.
(35) Franz, D. A.; Grimes, R. N. *J. Am. Chem. Soc.* **1971**, *93*, 387.
(36) Küpper, S.; Paetzold, P.; Boese, R. *Chem. Ber.* **1993**, *126*, 1787.

conditions far different from those common in carborane-forming reactions. Nevertheless, inorganic acetylene analogs may prove important in studying carborane-forming reactions because the intermediates in the inorganic case may have greater stability (compared to reaction with acetylene) which might allow their characterization.

Method

All geometries were optimized at the MP2/6-31G(d) level.[37] Vibrational frequencies were determined at that level to determine the nature of the potential energy surface and to make zero-point corrections (frequencies weighted by a 0.95 factor). Single-point calculations were made at the MP4/6-31G(d) and MP2/6-311+G(d,p) levels and combined[38] to estimated relative energies at the [MP4/6-311+G(d,p)] level, which, when zero-point corrections have been added, will constitute the "standard" level. All MP2 and MP4 calculations were made with the "frozen-core" approximation.

Heat capacities and entropy corrections were made using unscaled frequencies and standard statistical procedures[39] to determine enthalpies and free energies at 298 K. Free energies at 500 K were estimated from eq 8.

$$\Delta G(500\text{K}) \approx \Delta H(298\text{K}) - 500 \cdot \Delta S(298\text{K}) \qquad (8)$$

In cases where the reactant and product from a given transition structure were not clear, an IRC was constructed[40] at the MP2/6-31G(d) level. Molecular plots are given in Figure 1. A table of total energies (hartrees) and zero-point energies (kcal/mol) as well as **Z**-matrices of all structures are provided as supporting information. In addition, vibrational frequencies and intensities of several of the stable carborane structures are also provided as supporting information in the hopes that it may aid in the spectral identification.

A boldface notation system is used for some of the species in the figures, tables, and text to aid in identification. For example, the bold notation **TS2/3** refers to the transition state between structures **2** and **3**, while the notation **TS2/4+H$_2$** refers to the transition state for loss of H_2 from **2** to form **4**. Relative energies (kcal/mol) are presented in Table 1 with respect to the top entry in each section of structures. In Table 2, enthalpies at 298 K and free energies at 298 and 500 K are tabulated relative to $B_4H_{10} + C_2H_2$ which is given a value of zero. A potential energy diagram of enthalpies at 298 K is given in Figure 2 for the reaction path from $B_4H_{10} + C_2H_2$ to the products 1,2-$C_2B_3H_5$ + BH_3 + $2H_2$.

Results and Discussion

Addition of BH$_3$ and B$_2$H$_6$ to C$_2$H$_2$. A π-complex (**6a**) is calculated to be 3.3 kcal/mol more stable than separated BH_3 plus C_2H_2 and has a rotational barrier of less than 0.1 kcal/mol (**6b**). The transition state for hydrogen migration (**TS6/7**) is predicted to be very early with a forming C−H hydrogen distance of 1.714 Å and an activation barrier of 2.0 kcal/mol with respect to the π-complex (**6a**). The product (**7**) is 43.6 kcal/mol more stable than $BH_3 + C_2H_2$.

The addition of B_2H_6 to C_2H_2 requires a disruption of a B−H−B bridge before a π-complex (**8a**) can form. At the MP2/6-31G(d) level, the transition state **TS1+C$_2$H$_2$/8** (0.3 kcal/mol above **8a**) is characterized by very long C≡C to boron distances (2.000 and 2.014 Å). The C_1 minimum (**8a**) for the π-complex is slightly more stable than a symmetrical structure (**8b**) with the C−C bond perpendicular to the B−B axis. However, the energetic advantage of the C_1 structure over the C_s structure disappears after zero-point corrections are added. In fact, the existence of the π-complex is called into question since the transition state for forming the complex (**TS1+C$_2$H$_2$/8**) is predicted to have a lower energy at our standard level than the π-complex itself (**8a**). The transition state is 2.3 kcal/mol higher for migrating a hydrogen to carbon (**TS8/9**) than the π-complex **8a** (26.8 kcal/mol with respect to C_2H_2 plus B_2H_6) and closely resembles the corresponding C_2H_2−BH_3 transition state (**TS6/7**) with another BH_3 unit complexed to one B−H hydrogen. The product, a vinyl-substituted diborane (**9**), is predicted to be 29.7 kcal/mol more stable than $B_2H_6 + C_2H_2$.

For reference, the energy of $C_2H_2 + 2BH_3$ is included in Table 1 which allows the BH_3 binding energy to be compared at various levels. At our standard level, the B_2H_6 binding energy of 35.6 kcal/mol is in good agreement with experiment (36.5 ± 2.5 kcal/mol)[41] and previous experimental studies.[42]

While B_2H_6 is predicted to react with C_2H_2 via **TS8/9** at lower temperature, at 298 K, the two-step mechanism becomes competitive, namely:

	$\Delta G^{\ddagger}$(298K)
two-step	
$B_2H_6 \rightarrow 2BH_3$	26.7
$2BH_3 + C_2H_2 \rightarrow H_2BCH{=}CH_2 + BH_3$	7.7 ($BH_3 + C_2H_2 \rightarrow$ **TS6/7**)
total	34.4
one-step	
$B_2H_6 + C_2H_2 \rightarrow H_2B_2CH{=}CH_2$	35.5 ($B_2H_6 + C_2H_2 \rightarrow$ **TS8/9**)

Calculations on isolated B_3H_7[43] were made to determine relevant unimolecular rearrangement pathways. The most stable form of free B_3H_7 is the double-bridged (styx-2102[44]) form (**2**) followed by the styx-1103 form (**3**) which is 3.3 kcal/mol higher in energy (see Figure 1). A transition state connecting the two structures (**TS2/3**) has an activation barrier of 5.6 kcal/mol.

The lowest activation barrier (43.3 kcal/mol) for elimination of H_2 from **2** involves the simultaneous loss of two hydrogen bridges (**TS2/4+H$_2$**). A direct pathway for H_2 loss from the styx-2102 structure to the B_3H_5 global minimum (a three-membered ring with two bridging hydrogens) is blocked by a HOMO-LUMO crossing. In a paper comparing B_3H_n species, Korkin, McKee, and Schleyer[45] have calculated that **4** is 22.3 kcal/mol above the global minimum at the QCISD(T)/6-311+G(d,p) level. While it is likely that the B_3H_5 (**4**) will react without activation with C_2H_2 to form $C_2B_3H_7$ (donor−acceptor interaction between C_2H_2 π-orbital and symmetric combination of BH_2 empty orbitals), such a pathway is not likely due to the additional activation required to form B_3H_5 from B_3H_7.

(37) Frisch, M. J.; Trucks, G. W.; Schlegel, H. B.; Gill, P. M. W.; Johnson, B. G.; Wong, M. W.; Foresman, J. B.; Robb, M. A.; Head-Gordon, M.; Replogle, E. S.; Gomperts, R.; Andres, J. L.; Raghavachari, K.; Binkley, J. S.; Gonzalez, C.; Martin, R. L.; Fox, D. J.; Defrees, D. J.; Baker, J.; Stewart, J. J. P.; Pople, J. A. Gaussian92/DFT (Rev. G.2), Gaussian, Inc., Pittsburgh, PA, 1993.

(38) (a) McKee, M. L.; Lipscomb, W. N. *J. Am. Chem. Soc.* **1981**, *103*, 4673. (b) Nobes, R. H.; Bouma, W. J.; Radom, L. *Chem. Phys. Lett.* **1982**, *89*, 497. (c) McKee, M. L.; Lipscomb, W. N. *Inorg. Chem.* **1985**, *24*, 762.

(39) McQuarrie, D. A. *Statistical Thermodynamics*; Harper & Row: New York, 1973.

(40) McKee, M. L.; Page, M. Computing Reaction Pathways on Molecular Potential Energy Surfaces. In *Review in Computational Chemistry*; Lipkowitz, K. B., Boyd, D. B., Eds.; VCH, New York, 1993; Vol. 4, pp 35−65.

(41) Ruscic, B.; Mayhew, C. A.; Berkowitz, J. *J. Chem. Phys.* **1988**, *88*, 5580.

(42) (a) Page, M.; Adams, G. F.; Binkley, J. S.; Melius, C. F. *J. Phys. Chem.* **1987**, *91*, 2675. (b) Curtiss, L. A.; Pople, J. A. *J. Chem. Phys.* **1988**, *89*, 4875. (c) Stanton, J. F.; Bartlett, R. J.; Lipscomb, W. N. *Chem. Phys. Lett.* **1987**, *138*, 525. (d) Defrees, D. J.; Raghavachari, K.; Schlegel, H. B.; Pople, J. A.; Schleyer, P. v. R. *J. Phys. Chem.* **1987**, *91*, 1857. (e) Sana, M.; Leroy, G.; Henriet, Ch. *THEOCHEM* **1989**, *187*, 233. (f) Lammertsma, K.; Leszczynski, J. *J. Phys. Chem.* **1990**, *94*, 2806.

(43) For previous calculations on B_3H_7 see: (a) Stanton, J. F.; Lipscomb, W. N.; Bartlett, R. J. *J. Am. Chem. Soc.* **1989**, *111*, 5165. (b) Cioslowski, J.; McKee, M. L. *J. Phys. Chem.* **1992**, *96*, 9264.

(44) For styx notation see: Eberhardt, W. H.; Crawford, B. L., Jr.; Lipscomb, W. N. *J. Chem. Phys.* **1954**, *22*, 989.

(45) Korkin, A. A.; McKee, M. L.; Schleyer, P. v. R. *Inorg. Chem.* **1995**, *34*, 961.

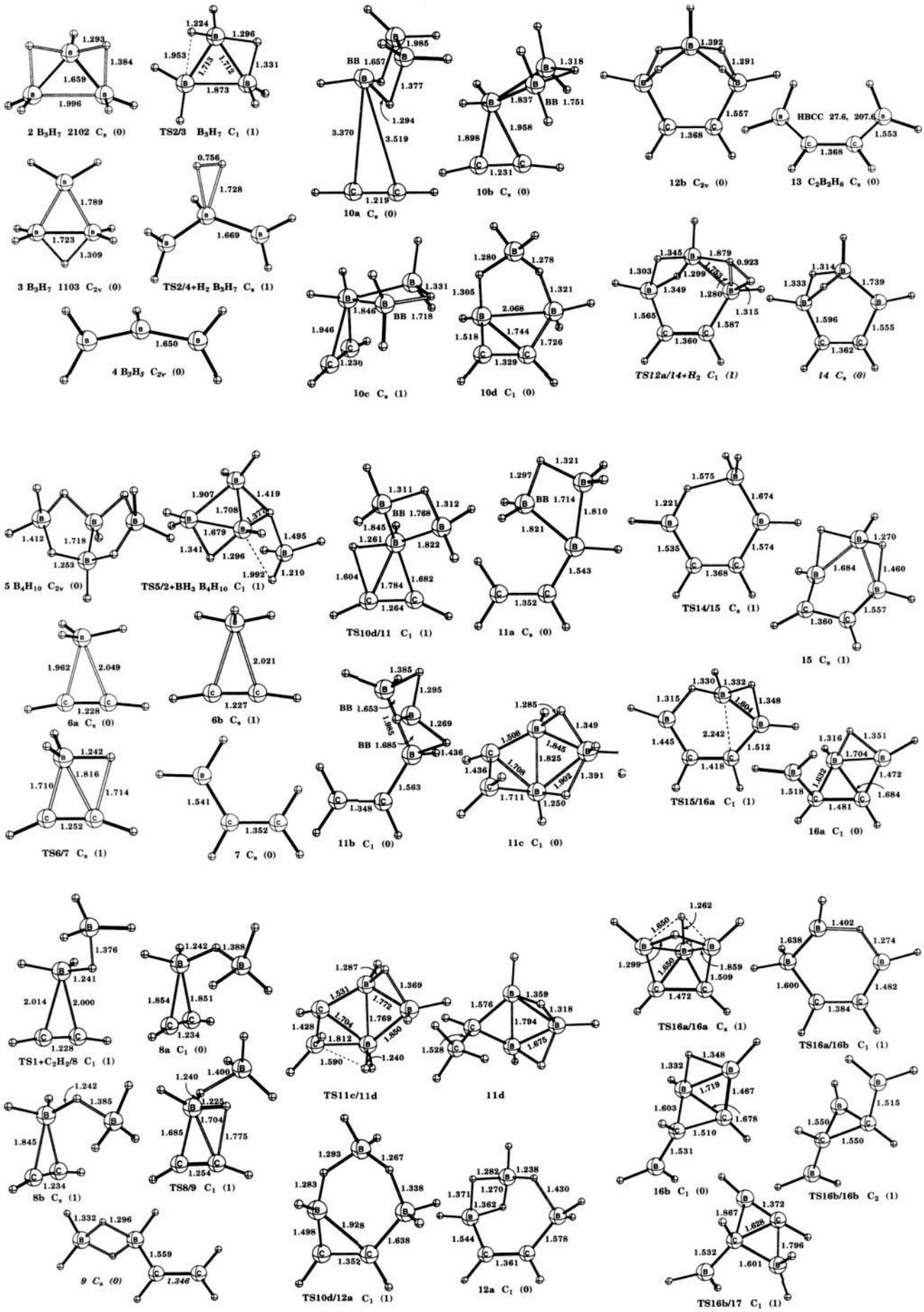
2 B_3H_7 2102 C_s (0)
TS2/3 B_3H_7 C_1 (1)
10a C_s (0)
10b C_s (0)
12b C_{2v} (0)
13 $C_2B_2H_6$ C_s (0)
HBCC 27.6, 207.6
3 B_3H_7 1103 C_{2v} (0)
TS2/4+H_2 B_3H_7 C_s (1)
4 B_3H_5 C_{2v} (0)
10c C_s (1)
10d C_1 (0)
TS12a/14+H_2 C_1 (1)
14 C_s (0)
5 B_4H_{10} C_{2v} (0)
TS5/2+BH_3 B_4H_{10} C_1 (1)
TS10d/11 C_1 (1)
11a C_s (0)
TS14/15 C_s (1)
15 C_s (1)
6a C_s (0)
6b C_s (1)
TS6/7 C_s (1)
7 C_s (0)
11b C_1 (0)
11c C_1 (0)
TS15/16a C_1 (1)
16a C_1 (0)
TS1+C_2H_2/8 C_1 (1)
8a C_1 (0)
TS11c/11d
11d
TS16a/16a C_s (1)
TS16a/16b C_1 (1)
8b C_s (1)
TS8/9 C_1 (1)
9 C_s (0)
TS10d/12a C_1 (1)
12a C_1 (0)
16b C_1 (0)
TS16b/16b C_2 (1)
TS16b/17 C_1 (1)

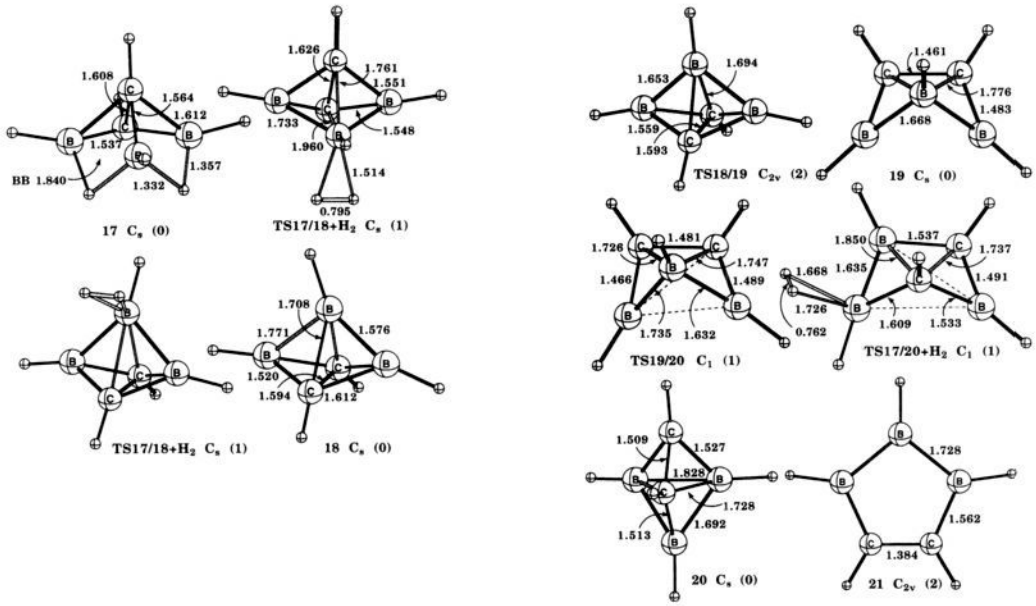

Figure 1. Selected geometric parameters of species optimized at the MP2/6-31G(d) level. The same boldface notations are used in the tables and text. Symmetry point group designations are given as well as the number of imaginary frequencies at the MP2/6-31G(d) level (in parentheses).

$B_4H_{10} \rightarrow B_3H_7 + BH_3$. The transition state for B_4H_{10} (**5**) $\rightarrow$ B_3H_7 (**2**) + BH_3 **TS5/2+BH$_3$** (located at the MP2(FC)/6-31G-(d) level) is essentially identical to the structure calculated previously[46] at the MP2(FULL)/6-31G(d) level. At our standard level, the activation barrier is 37.6 kcal/mol which is very similar to the value of 35.1 kcal/mol calculated at the [MP4/6-311G-(d,p)]+ZPC/6-31G(d) level.[46]

$B_3H_7 + C_2H_2$. Four different π-complex structures were considered between B_3H_7 and C_2H_2. The double-bridged (2102) B_3H_7 (**2**) forms a weak π-complex with C_2H_2 (**10a**), bound by 1.6 kcal/mol with respect to B_3H_7 (**2**) + BH_3. The higher-energy single-bridged (1103) B_3H_7 (**3**) forms a slightly stronger (binding energy is 2.3 kcal/mol with respect to (1103) B_3H_7 (**3**) + C_2H_2) π-complex with C_2H_2 (**10b**) which is 2.6 kcal/mol less stable than **10a**. Rotating the C_2H_2 moiety in **10b** by 90° yields **10c**, a structure with nearly the same energy as **10b** but having one imaginary frequency.[47] When **10c** was allowed to optimize without symmetry constraints, a new structure, **10d**, was obtained which was quite different from **10a**−**c**. One of the interesting characteristics is the nearly full conversion of the acetylenic group into an olefinic group. The best description of changes is by analogy to the addition of B−H across the C≡C triple bond (Figure 3). The in-plane π component of acetylene donates charge into the vacant p-orbital on boron while the in-plane π^* component accepts charge from the BH σ orbital (Figure 3a). In analogy with BH_3, the nearly vacant orbital on boron of B_3H_7 accepts charge from acetylene while the occupied BBB three-center bond plays the role of a BH σ orbital and donates charge into the π^* orbital of acetylene (Figure 3b). In the rearrangement, there is a concurrent transformation of a BH terminal hydrogen into a BH bridging hydrogen. Thus, as boron adds to one side of the triple bond, the three-center BBB bond is converted to a three-center BBC bond. The addition product (**10d**) is 6.6 kcal/mol more stable than B_3H_7 plus C_2H_2.

A transition state of C_1 symmetry (**TS10d/11**) was located for hydrogen migration from boron to carbon in the π-complex. Even though the transition state resembles **10b/10c**, the reactant in the transformation must be **10d** on the MP2/6-31G(d) potential energy surface, because the energy of the transition state (**TS10d/11**) at the MP2/6-31G(d) level is below the energy of all other π-complexes (Table 1). With respect to **10d**, the activation barrier at the standard level is 6.4 kcal/mol. The product of reaction is **11a**, a vinyl derivative of B_3H_7 **3**, which is 32.3 kcal/mol lower in energy than **10d**. Since B_3H_7 **2** is lower in energy than B_3H_7 **3** by 3.3 kcal/mol, it comes as no surprise that the vinyl derivative of B_3H_7 **2** (**11b**) is 1.1 kcal/mol lower in energy than **11a**. Given the small activation barrier for conversion of **3** $\rightarrow$ **2** (2.3 kcal/mol), the rearrangement **11a** $\rightarrow$ **11b** should be facile.

When a vinyl group is substituted for a basel terminal hydrogen in **3**, extensive geometry reorganization occurs to give **11c**, which is 4.7 kcal/mol more stable than **11a** and 3.6 kcal/mol more stable than **11b**. The C=C π bond is interacting extensively with boron in **11c** as shown by the longer C=C bond (1.436 Å) compared to **11a** (1.352 Å) or **11b** (1.348 Å). Rearrangement barriers among the **11a**, **11b**, and **11c** structures should be small.

From **11c**, there is only a small activation barrier (3.0 kcal/mol) for the migration of a bridging hydrogen to the methylene carbon (**TS11c/11d**), forming an exocyclic methyl group. This methyl-substituted *nido*-carborane (**11d**) is 13.0 kcal/mol more stable than **11c** and, in fact, is the global minimum on the $C_2B_3H_9$ potential energy surface.

Experimentally, it is known[35] that B_4H_{10} + C_2H_2 yields methylated carboranes including 2-CH_3-2,3,4-$C_3B_3H_6$. A possible mechanism for formation of this product would be eqs 9 and 10.

$$B_3H_7 + C_2H_2 \rightarrow CH_3{-}CB_3H_6\ (\mathbf{11d}) \qquad (9)$$

$$CH_3{-}CB_3H_6\ (\mathbf{11d}) + C_2H_2 \rightarrow CH_3{-}C_3B_3H_8 \rightarrow CH_3{-}C_3B_3H_6 + H_2 \qquad (10)$$

(46) (a) McKee, M. L. *J. Am. Chem. Soc.* **1990**, *112*, 6753. (b) An error has been discovered in Table III of reference 46a for the reaction $B_4H_{10} \rightarrow B_4H_8 + H_2$ at the MP2/6-311G(d,p) level. The reported barrier at that level, 31.3 kcal/mol, is incorrect. The correct barrier, computed from the absolute energies in Table 2,[46a] is 39.2 kcal/mol. As a consequence, the two pathways for unimolecular decomposition of B_4H_{10} (to B_3H_7 plus BH_3 and to B_4H_8 plus H_2) are much closer together than previously reported.[46a]

(47) The transition vector for **10c** (87i cm^{-1}) is more complicated than a simple rotation of the C_2H_2 group. There is also a tilt of the C_2H_2 group toward the unique boron.

Table 1. Relative Energies, Enthalpies, and Free Energies (kcal/mol) of Various Species

	relative energies[a]					thermodynamic values (298 K)[d]	
	MP2/a	MP4/a	MP2/b	[MP4/b][b]	+ZPC[c]	ΔH	ΔG
$BH_3 + C_2H_2$	0.0	0.0	0.0	0.0	0.0	0.0	0.0
6a	−7.3	−6.5	−7.4	−6.6	−3.3	−3.9	4.1
6b	−7.1	−6.3	−7.3	−6.5	−3.3	−4.3	4.7
TS6/7	−5.0	−4.7	−5.3	−5.0	−1.3	−2.7	7.1
7	−50.8	−51.5	−49.6	−50.3	−43.6	−44.8	−35.5
B_2H_6 (**1**) + C_2H_2	0.0	0.0	0.0	0.0	0.0	0.0	0.0
TS1+C_2H_2/8	23.5	24.3	23.2	24.0	24.3	24.3	32.4
8a	23.2	24.2	23.0	24.0	24.5	24.6	32.5
8b	23.3	24.2	23.2	24.1	24.5	24.1	33.3
TS8/9	25.6	26.1	25.5	26.0	26.8	26.3	35.5
9	−45.4	−36.3	−44.4	−35.3	−29.7	−30.5	−20.7
$2BH_3 + C_2H_2$	40.4	40.5	42.1	42.2	35.6	37.0	26.7
B_3H_7 (**2**)	0.0	0.0	0.0	0.0	0.0	0.0	0.0
TS2/3	7.3	7.0	7.1	6.8	5.6	5.6	5.7
B_3H_7 (**3**)	4.4	4.2	4.4	4.2	3.3	3.5	3.6
TS2/4+H_2	53.3	51.7	50.7	49.1	43.3	44.3	42.4
B_3H_5 (**4**) + H_2	47.4	45.0	48.8	46.4	37.3	39.3	29.5
B_4H_{10} (**5**)	0.0	0.0	0.0	0.0	0.0	0.0	0.0
TS5/2+BH_3	45.4	43.2	43.5	41.3	37.6	38.2	36.3
B_3H_7 (**2**) + BH_3	40.1	38.2	41.8	39.9	34.4	35.6	23.5
B_3H_7 (**2**) + C_2H_2	0.0	0.0	0.0	0.0	0.0	0.0	0.0
π-complex (**10a**)	−2.1	−1.9	−2.3	−2.1	−1.6	−0.5	4.6
π-complex (**10b**)	−3.3	−1.2	−3.6	−1.5	1.0	1.2	11.4
π-complex (**10c**)	−3.3	−1.5	−3.5	−1.7	0.1	0.6	11.4
π-complex (**10d**)	−12.6	−11.0	−12.7	−11.1	−6.6	−7.3	3.9
TS10d/11	−4.6	−2.0	−5.2	−2.6	−0.2	−1.0	10.5
11a	−45.0	−45.4	−43.7	−44.1	−38.9	−39.4	−29.2
11b	−46.1	−46.3	−45.3	−45.5	−40.0	−40.7	−29.8
11c	−55.9	−51.9	−54.5	−50.5	−43.6	−45.0	−32.5
TS11c/11d	−50.7	−46.9	−50.2	−46.4	−40.6	−42.1	−29.4
11d	−68.7	−66.3	−66.7	−64.3	−56.6	−57.8	−45.8
TS10d/12a	−11.7	−11.2	−12.3	−11.8	−7.6	−8.6	2.9
12a	−44.5	−44.5	−45.2	−45.2	−39.3	−40.5	−28.5
12b	−43.9	−42.7	−46.6	−45.4	−39.7	−41.2	−28.2
$C_2B_2H_6$ (**13**) + BH_3	−7.7	−8.0	−4.5	−4.8	−5.9	−5.1	−6.7
TS12a/14+H_2	−22.2	−21.3	−26.6	−25.7	−21.8	−23.3	−10.7
14 + H_2	−24.1	−25.0	−23.9	−24.8	−25.4	−25.3	−22.3
14	0.0	0.0	0.0	0.0	0.0	0.0	0.0
TS14/15	18.3	17.4	19.3	18.4	15.6	16.1	15.0
15	−11.8	−10.2	−10.1	−8.5	−8.8	−9.0	−8.3
B_3H_5 (**4**) + C_2H_2	71.5	69.9	72.7	71.1	62.6	64.5	51.7
TS15/16a	40.8	40.5	39.6	39.3	37.5	37.6	37.2
16a	−12.3	−8.3	−9.8	−5.8	−6.0	−6.0	−5.8
TS16a/16a	−3.8	1.7	−4.7	0.8	−0.4	−0.9	0.4
TS16a/16b	44.0	42.6	43.3	41.9	38.9	39.2	39.6
16b	−7.5	−3.9	−5.0	−1.4	−1.9	−1.8	−1.8
TS16b/16b	7.0	10.2	9.1	12.3	9.4	9.8	9.3
TS16b/17	34.5	38.4	33.8	37.7	34.3	34.9	34.0
17	−28.5	−22.6	−26.2	−20.3	−19.3	−19.9	−18.4
TS17/18+H_2	57.9	64.2	55.9	62.2	58.4	58.4	59.0
TS17/20+H_2	41.8	44.9	40.2	43.3	39.2	39.5	39.4
18 + H_2	27.0	33.4	29.9	36.3	28.0	29.5	20.8
18	0.0	0.0	0.0	0.0	0.0	0.0	0.0
TS18/19	0.3	0.6	0.4	0.7	0.2	−0.5	1.1
19	−6.9	−9.7	−6.8	−9.6	−8.3	−8.5	−8.2
TS19/20	−5.8	−8.2	−5.9	−8.3	−7.3	−7.9	−7.0
20	−23.4	−23.9	−22.5	−23.0	−21.6	−22.1	−21.2
21	20.3	12.4	19.1	11.2	11.8	11.0	12.4

[a] Basis set a is 6-31G(d). Basis set b is 6-311+G(d,p). [b] Values computed with additivity approximation. ΔE[MP4/b] = ΔE(MP4/a) + ΔE(MP2/b) − ΔE(MP2/a). [c] Zero-point correction made by weighting zero-point energies by a 0.95 factor. [d] Thermodynamic corrections have been computed with MP2/6-31G(d) vibrational frequencies.

Thus, the reactive species **11d** might be trapped by the addition of a second molecule of acetylene.

Turning back to addition products, a second transition state (**TS10d/12a**) was located for transformation of **10d** into an open cyclic system (**12a**). As the transition state is approached a 3c−2e BBC bond is converted into a BC bond, while after the transition state, a terminal BH is converted into a BH bridge (Figure 4). A second cyclic form (**12b**) was located which featured an interesting pentacoordinate boron. In this regard it is interesting to note that a structure of B_3H_9 with a very similar pentacoordinate boron was calculated by Schaefer and coworkers[48] and found to be only 3.5 kcal/mol higher than the more conventional C_{3v} structure (Figure 5). In fact, **12b** is related to the higher-energy form of B_3H_9 by replacing two

Table 2. Enthalpies and Free energies (kcal/mol) Relative to $B_4H_{10} + C_2H_2$

	relative thermodynamic values		
	ΔH (298 K)	ΔG (298 K)	ΔG (500 K)
B_4H_{10} (**5**) + C_2H_2	0.0	0.0	0.0
TS5/2+BH$_3$ + C_2H_2	38.2	36.3	35.0
2 + C_2H_2, BH_3	35.6	23.5	15.2
10a	35.1	28.1	23.2
10b	36.8	34.9	33.6
10c	36.2	34.9	33.7
10d	28.3	27.4	26.7
TS10d/11	34.6	34.0	33.5
11a	−3.8	−5.7	−7.0
11b	−5.1	−6.3	−7.2
11c	−9.4	−9.0	−8.8
TS11c/11d	−6.5	−5.9	−5.6
11d	−22.2	−22.3	−22.4
TS10d/12a	27.0	26.4	25.9
12a	−4.9	−5.0	−5.1
12b	−5.9	−4.7	−4.2
$C_2B_2H_6$ (**13**) + 2BH_3	30.5	16.8	7.4
TS12a/14+H$_2$	12.3	12.8	13.0
14, H_2	10.3	1.2	−5.1
TS2/4+H$_2$ + C_2H_2, BH_3	79.8	65.8	43.3
4 + C_2H_2, BH_3, H_2	74.8	52.9	38.0
TS14/15 + BH_3, H_2	26.4	16.2	9.1
15 + BH_3, H_2	1.3	−7.1	−12.9
TS15/16a + BH_3, H_2	47.9	34.4	31.8
16a + BH_3, H_2	4.3	−4.6	−10.7
TS16a/16a + BH_3, H_2	9.4	1.6	−3.8
TS16a/16b + BH_3, H_2	49.5	40.8	34.7
16b + BH_3, H_2	8.5	−0.6	−6.9
TS16b/16b + BH_3, H_2	20.1	10.5	3.7
TS16b/17 + BH_3, H_2	45.2	35.2	28.4
17 + BH_3, H_2	−9.6	−17.2	−22.5
TS17/18 + **H$_2$** + BH_3	68.7	60.2	54.3
TS17/20 + **H$_2$** + BH_3	49.8	40.6	34.3
18 + BH_3, 2H_2	39.8	22.0	9.7
TS18/19 + BH_3, 2H_2	39.3	23.1	11.9
19 + BH_3, 2H_2	31.3	13.8	1.6
TS19/20 + BH_3, 2H_2	31.9	15.0	3.3
20 + BH_3, 2H_2	17.7	0.8	−10.9
21 + BH_3, 2H_2	50.8	43.3	23.1

terminal BH bonds with the −HC=CH− group. It should be noted that both **12a** and **12b** are minima (no imaginary frequencies); **12a** is slightly lower in energy at the MP2/6-31G(d) level, while **12b** is slightly lower at the standard level.

If **12b** loses a BH_3 from the pentacoordinate position, $C_2B_2H_6$ (**13**) is obtained. While **13** is not the global minimum on the $C_2B_2H_6$ potential energy surface (structures with a bridging methylene group are more stable),[49,50] the structure considered here (**13**) is likely to be the initial product of BH_3 loss from **12b** and therefore allows an estimate to be made of the activation barrier for loss of BH_3 (33.8 kcal/mol).

The second obvious decomposition pathway from **12a** or **12b** is loss of H_2. While several mechanisms for H_2 loss were considered from $C_2B_3H_9$ (**12a/12b**), only one transition state (**TS12a/14+H$_2$**) could be located. In the transition state, the terminal and bridging hydrogens are eliminated from the same center with the concurrent formation of a BB bond in the product (**14**). The forward activation barrier for the process is 17.5 kcal/mol, while the reverse barrier is only 3.6 kcal/mol. The intermediate, **14**, resembles a *cis*-substituted ethylene RHC=CHR′, where R = BH_2 and R′ = $BHBH_2$. Another way to view **14** is as a substituted diborane where a terminal hydrogen on each boron is replaced with a bridging −CH=CH−HB− group. Such diborane derivatives are known when the bridging group is −NR−BH−RN−.[51] If one hydrogen bridge is broken, a transition state (**TS14/15**) is reached (activation barrier is 15.6 kcal/mol) for formation of another cyclic system (**15**) which is 8.8 kcal/mol lower than **14**. Structure **15** is known as a ligand for iron complexes.[52]

A much more direct path to **15** would be $B_3H_5 + C_2H_2 \rightarrow$ **15**, which is 71.4 kcal/mol exothermic. However, the high activation barrier to form B_3H_5 from B_3H_7 (**TS2/4+H$_2$**, 43.3 kcal/mol) precludes this pathway.

The only well-characterized structure on the $C_2B_3H_7$ surface is the *nido*-carborane (**17**), where a carbon caps a square base of borons.[53-56] While many attempts were made to connect **15** and **17** with a single transition state, none was successful. Instead, two intervening intermediates were located (**16a**, **16b**). In the first phase, the C=C double bond is converted into a C−C single bond as the transition state (**TS15/16a**) is reached (CC 1.360 Å (**15**) → 1.418 Å (**TS15/16a**) → 1.481 Å (**16a**)). From **16a**, a transition state (**TS16a/16b**) is reached to a closely related intermediate (**16b**). The two structures, **16a** and **16b**, bare some resemblance to the global minimum on the $C_2B_2H_4$ surface (methyleneborane[50]), found by Schleyer and co-workers[57] and by Schaefer and co-workers,[58] with two differences: the C=B bond is saturated and a BH_2 unit replaces a hydrogen on the methylene carbon.

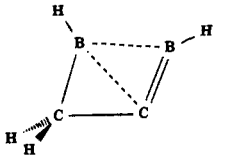

nonclassical methyleneborane

The activation barrier for reaching **TS16a/16b** from **16a** is quite large (44.9 kcal/mol). The motion required can be visualized as the exchange of the two substituents on the methylene carbon (H and BH_2) which takes place by a rotation of the methylene group.

The intermediates **16a** and **16b** are both fluxtional as indicated by the low barriers for **16a** → **16a** (through **TS16a/16a**; 5.6 kcal/mol) and **16b** → **16b** (through **TS16b/16b**; 11.3 kcal/mol). On the other hand, much higher barriers exist from **15** (through **TS15/16a**; 43.5 kcal/mol) and **16b** (through **TS16b/17**; 36.2 kcal/mol). The latter transition state (**TS16b/17**) is particularly interesting as it features a very short C−B bond (1.372 Å) with definite double bond character. All of the structures from **15** to **17** show a gradual increase in the C−C distance (**15** → **TS15/16a** → **16a** → **16b** → **TS16b/17** → **17**; 1.360 → 1.418 → 1.481 → 1.510 → 1.601 → 1.608 Å),

(48) Duke, B. J.; Liang, C.; Schaefer, H. F. *J. Am. Chem. Soc.* **1991**, *113*, 2884.
(49) Willershausen, P.; Schmidt-Lukasch, G.; Kybart, C.; Allwohn, J.; Massa, W.; McKee, M. L.; Schleyer, P. v. R.; Berndt, A. *Angew. Chem., Int. Ed. Engl.* **1992**, *31*, 1384.
(50) Berndt, A. *Angew. Chem., Int. Ed. Engl.* **1993**, *32*, 985.
(51) Müller, M.; Wagner, T.; Englert, U.; Paetzold, P. *Chem. Ber.* **1995**, *128*, 1.
(52) (a) Sneddon, L. G.; Beer, D. C.; Grimes, R. N. *J. Am. Chem. Soc.* **1973**, *95*, 6623. (b) Spencer, J. T.; Grimes, R. N. *Organometallics* **1987**, *6*, 323.
(53) Onak, T. In *Comprehensive Organometallic Chemistry*; Wilkinson, G., Stone, F. G. A., Abel, E., Eds.; Pergamon: Oxford, England, 1982; Vol. 1, pp 411−457.
(54) McKee, M. L. *Inorg. Chem.* **1988**, *27*, 4241.
(55) Bühl, M.; Schleyer, P. v. R. *J. Am. Chem. Soc.* **1992**, *114*, 477.
(56) Schleyer, P. v. R.; Gauss, J.; Bühl, M.; Greatrex, R.; Fox, M. A. *J. Chem. Soc., Chem. Commun.* **1993**, 1766.
(57) (a) Budzelaar, P. H. M.; Schleyer, P. v. R.; Krogh-Jespersen, K. *Angew. Chem., Int. Ed. Engl.* **1984**, *23*, 825. (b) Budzelaar, P. H. M.; Krogh-Jespersen, K.; Clark, T.; Schleyer, P. v. R. *J. Am. Chem. Soc.* **1985**, *107*, 2773.
(58) Frenking, G.; Schaefer, H. F. *Chem. Phys. Lett.* **1984**, *109*, 521.

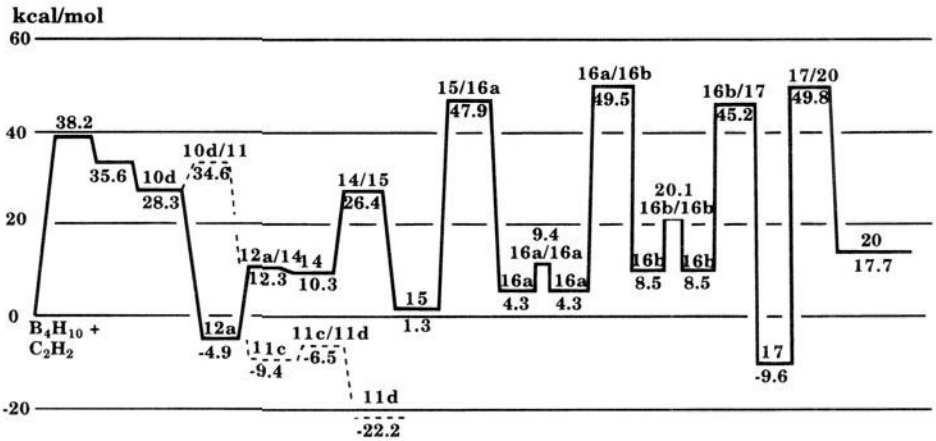

Figure 2. Potential energy diagram of enthalpies at 0 K with respect to $B_4H_{10} + C_2H_2$. The solid line indicates the preferred pathway for formation of 1,2-$C_2B_3H_5 + BH_3 + 2H_2$. The dotted line **10d** → **11c** → **11d** is the hydroboration pathway to a methyl-substituted *nido*-carborane (**11d**).

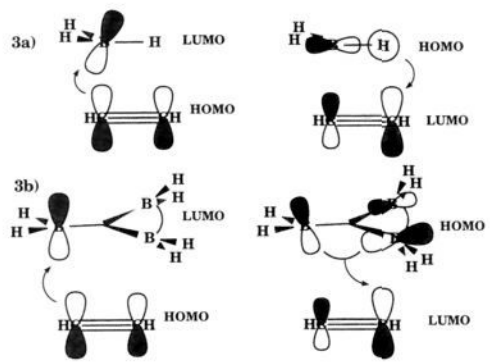

Figure 3. Schematic diagram showing the analogous donor−acceptor (HOMO-LUMO) interactions in the addition of BH_3 and B_3H_7 to C_2H_2. (a) B−C and C−H bonds are formed, and a B−H bond is broken in the addition of BH_3 to HC≡CH. (b) A B−C bond is formed and a BBB 3c−2e bond is converted into a BBC 3c−2e bond in the addition of B_3H_7 to HC≡CH.

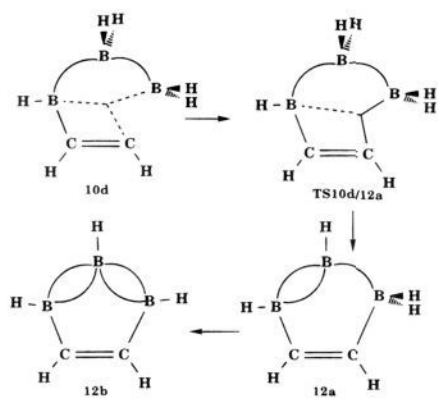

Figure 4. Schematic diagram showing the transformation of **10d** into **12b**. In the first step, a BBC 3c−2e bond is converted into a CB bond. In the second and third steps, terminal to bridge conversions are made.

indicating smooth transition from a C=C double bond to one *involving multicenter bonding*.

As mentioned above, structure **17** is the only $C_2B_3H_7$ carborane which has been characterized and several calculations on its structure and properties (e.g. IR spectra and chemical shifts) have been reported.[54−56] At the MP2/6-31G(d)//MP2/6-31G(d)+ZPC level Bühl and Schleyer[55] reported that **17** was 16.6 kcal/mol more stable than **15**, somewhat higher than the present value of 10.5 kcal/mol. The geometries

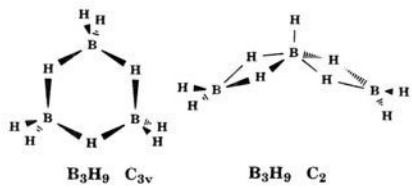

Figure 5. Illustration of two structures of B_3H_9 (C_{3v} and C_2). The pentacoordinate boron in the C_2 structure, which is only 3.5 kcal/mol higher in energy than the C_2 structure,[48] is very similar to the corresponding boron in **12b**.

reported by Bühl and Schleyer for **17** are also slightly different because they optimized geometries with MP2 (FULL) while the present values are with MP2 (FC) (e.g. including all orbitals in computing the MP2 energy and gradients (FULL), versus freezing the core orbitals (FC)).

Two transition states (**TS17/18+H_2, TS17/20+H_2**) have been located for the elimination of H_2 from $C_2B_3H_7$. The higher-energy transition state **TS17/18+H_2** of C_s symmetry has been presented twice in Figure 1 in order to more clearly show the relationship with the reactant (**17**) and the product (**18**). The transition state, formed by concerted elimination of both bridging hydrogens, is late as indicated by the short H−H distance (0.795 Å) and long B−H distances (1.514 Å). The forward activation barrier (77.7 kcal/mol) is the largest encountered on the potential energy surface, while the product **18** is a slightly distorted 2,3-$C_2B_3H_5$ trigonal bipyramid. If the 2,3-$C_2B_3H_5$ isomer is optimized in C_{2v} symmetry, the structure, while only 0.3 kcal/mol higher than **18** at the MP2/6-31G(d) level, is actually a stationary point of order two. Optimizing this structure (given the designation **TS18/19** despite having the wrong number of imaginary frequencies) in the direction of the largest imaginary frequency yields the minimum **19**, which bears an obvious resemblance to B_5H_{11}. Only a small distortion of **19** is required to reach **TS19/20** which is higher in energy by only 1.0 kcal/mol at the standard level. Since **18** (through **TS18/19**) and **19** (through **TS19/20**) have such small forward barriers, the reaction is essentially a nonsynchronous reaction for the formation of **20** from **17**. After much effort, a synchronous transition state (**TS17/20+H_2**) was located for the direct formation of **20** from **17**. The transition state resembles a distorted square pyramid with a carbon atom in the apical position. The loss of H_2 comes from one bridging hydrogen and one terminal hydrogen. The synchronous transition state (**TS17/20+H_2**) is 19.2 kcal/mol lower in energy than **TS17/18+H_2**. It should be emphasized that *both structures* are transition states (one imaginary fre-

quency) on the MP2/6-31G(d) potential energy surface. Planar 1,2-$C_2B_3H_5$ (**21**), provided for comparison, is 33.4 kcal/mol higher in energy than the 1,2-$C_2B_3H_5$ trigonal bipyramidal structure (**20**).

Mechanism of Carborane Formation

The underlying mechanism of carborane formation from a boron hydride and acetylene involves the initial decomposition of the boron hydride to form a reactive boron hydride which subsequently reacts with acetylene. The reactive boron hydride will have at least one low-lying acceptor orbital which can accept electrons from the acetylene π-orbital to form a donor–acceptor complex.

In the reaction of B_4H_{10} with acetylene, three different reactive boron hydrides may be formed, BH_3, B_3H_7, and B_4H_8. All three will react readily with acetylene and the exact course of the reaction will depend on a subtle balance of activation barriers, concentrations, and temperature. Reactions of BH_3 and B_3H_7 with acetylene are considered presently, while the reaction of B_4H_8 with acetylene will be considered in a separate paper.

The overall mechanism for formation of 1,2-$C_2B_3H_5$ from $B_3H_7 + C_2H_2$ is given below (eqs 11 and 12)

$$B_3H_7 + C_2H_2 \rightarrow \underset{\textbf{10d}}{C_2B_3H_9} \rightarrow \textbf{12a} \rightarrow \underset{\textbf{14}}{C_2B_3H_7} + H_2 \quad (11)$$

$$\underset{\textbf{14}}{C_2B_3H_7} \rightarrow \textbf{15} \rightarrow \textbf{16a} \rightarrow \textbf{16b} \rightarrow \textbf{17} \rightarrow \underset{\textbf{20}}{1,2\text{-}C_2B_3H_5} + H_2 \quad (12)$$

where only minima are indicated (Figure 2). The largest barrier is predicted for the **17** → **20** step (59.4 kcal/mol). Thermodynamic properties of all minima and transition states are compared with $B_4H_{10} + C_2H_2$ (which is given a reference of zero) in Table 2. Comparing enthalpies at 298 K, the four highest activation barriers are within 5 kcal/mol (47.9, 49.5, 45.2, and 49.8 kcal/mol). Interestingly, the activation barrier for forming $B_3H_7 + BH_3$ from B_4H_{10} (38.2 kcal/mol) is not the rate-determining step. Free energies at 298 and 500 K are also determined to see the effect of temperature on the mechanism (Table 2). At 500 K, the free energy of the transition state to form B_3H_7 (35.0 kcal/mol) is slightly larger than the free energy of the transition state for loss of H_2 from $C_2B_3H_7$ (34.3 kcal/mol). The free energy at 500 K for the elimination of H_2 from B_3H_7 **TS2/4+H$_2$** (and the subsequent addition of C_2H_2 to form **15**) is not competitive with the steps shown in Figure 2. However, at more elevated temperatures, the initial elimination of H_2 may be more favorable. The similarity of free energies perhaps explains why the composition of carborane products is dependent on temperature. Lower temperatures favor stable alkylboranes and *nido*-carboranes, while higher temperatures favor loss of hydrogen and formation of *closo*-carboranes.

Conclusions

An initial effort is made to unravel the complicated mechanism of carborane formation from boron hydrides plus acetylene by studying the reactions $B_3H_7 + C_2H_2 \rightarrow$ 1,2-$C_2B_3H_5 + 2H_2$. Several interesting discoveries have been made. First, the expected π-complex between B_3H_7 and C_2H_2 collapses without activation to an addition product. Next, the addition product preferentially rearranges to a cyclic system rather than undergo the hydroboration reaction. A series of steps leads initially to the cyclic $C_2B_3H_7$ structure, and then to the more compact (and stable) *nido*-$C_2B_3H_7$ cage. A rather high activation barrier separates the $C_2B_3H_7$ cage from the *closo*-carborane, 1,2-$C_2B_3H_5$. Four activation barriers lie in the range 45–50 kcal/mol above B_4H_{10} plus C_2H_2. At higher temperatures, the reaction is driven by entropy, while at lower temperatures, the reaction is controlled by the thermodynamic stability of products.

Under the appropriate experimental conditions it may be possible to trap and/or isolate several of the intermediates found here (**11d**, **12a/b**, **15**, **16a**, **16b**). It is hoped that this study will provide impetus to further research in carborane formation.

Acknowledgment. Computer time for this study was made available by the Alabama Supercomputer Network and the NSF-supported Pittsburgh Supercomputer Center. I thank Dr. Nico J. R. van Eikema Hommes for making Molecule available, which was used for drawing the structures in Figure 1.

Supporting Information Available: Tables of total energies (hartrees), zero-point energies (kcal/mol), calculated vibrational frequencies (cm^{-1}), and intensities (km/mol) and **Z**-matrices of the related species optimized at the MP2(FC)/6-31G(d) level (33 pages). This material is contained in many libraries on microfiche, immediately follows this article in the microfilm version of the journal, can be ordered from the ACS, and can be downloaded from the Internet; see any current masthead page for ordering information and Internet access instructions.

JA943985R